

# Spectrally Corrected Polynomial Approximation for Quantum Singular Value Transformation

Krishnan Suresh

University of Wisconsin–Madison, Madison, WI 53706, USA

Quantum Singular Value Transformation (QSVT) provides a unified framework for applying polynomial functions to the singular values of a block-encoded matrix. QSVT prepares a state proportional to  $\mathbf{A}^{-1}\mathbf{b}$  with circuit depth  $O(d \cdot \text{polylog}(N))$ , where  $d$  is the polynomial degree of the  $1/x$  approximation and  $N$  is the size of  $\mathbf{A}$ . Current polynomial approximation methods are over the continuous interval  $[a, 1]$ , giving  $d = O(\sqrt{\kappa} \log(1/\varepsilon))$ , and make no use of any properties of  $\mathbf{A}$ .

We observe here that QSVT solution accuracy depends only on the polynomial accuracy at the eigenvalues of  $\mathbf{A}$ . When all  $N$  eigenvalues are known exactly, a pure spectral polynomial  $p_S$  can interpolate  $1/x$  at these eigenvalues and achieve unit fidelity at reduced degree. But its practical applicability is limited. To address this, we propose a spectral correction that exploits prior knowledge of  $K$  eigenvalues of  $\mathbf{A}$ . Given any base polynomial  $p_0$ , such as Remez, of degree  $d_0$ , a  $K \times K$  linear system enforces exact interpolation of  $1/x$  only at these  $K$  eigenvalues without increasing  $d_0$ . The spectrally corrected polynomial  $p_{SC}$  preserves the continuous error profile between eigenvalues and inherits the parity of  $p_0$ .

QSVT experiments on the 1D Poisson equation demonstrate up to a  $5\times$  reduction in circuit depth relative to the base polynomial, at unit fidelity and improved compliance error. The correction is agnostic to the choice of base polynomial and robust to eigenvalue perturbations up to 10% relative error. Extension to the 2D Poisson equation suggests that correcting a small fraction of the spectrum may suffice to achieve fidelity above 0.999.

Krishnan Suresh: [ksuresh@wisc.edu](mailto:ksuresh@wisc.edu)

## 1 Introduction

Quantum Singular Value Transformation (QSVT), introduced by Gilyén et al. [1], provides a unified framework for applying polynomial functions to a matrix encoded as a quantum oracle [2]. Its most celebrated application is the quantum linear systems algorithm [3]: given a block encoding of a Hermitian positive definite (HPD) matrix  $\mathbf{A}$  of size  $N \times N$ , and a polynomial  $p$  of degree  $d$  approximating  $1/x$ , QSVT prepares a quantum state proportional to  $\mathbf{A}^{-1}\mathbf{b}$  with circuit depth  $O(d \cdot \text{polylog}(N))$ . All existing polynomial construction methods — the Remez minimax polynomial [4], the Mang truncated Chebyshev series [5], and analytical construction by Sundërhauf et al. [6] — treat the approximation over the *continuous* interval  $[a, 1]$ , where  $a = \lambda_{\min}(\mathbf{A})$ , giving degree  $O(\sqrt{\kappa} \log(1/\varepsilon))$  with  $\kappa = \lambda_{\max}/\lambda_{\min}$  and target accuracy  $\varepsilon$ . They make no use of any properties of  $\mathbf{A}$ .

In this paper, we investigate whether the *spectral* structure of  $\mathbf{A}$  can be exploited to improve the polynomial approximation. We show that if  $K \ll N$  eigenvalues of  $\mathbf{A}$  are known, either analytically or approximately, a simple correction to any base polynomial yields significant improvements in QSVT solution accuracy at no increase in circuit depth. Specifically, we derive a simple min-norm correction to any base polynomial by enforcing exact interpolation at  $K$  specified eigenvalues while minimizing the perturbation to the Chebyshev coefficients. The correction only requires a  $K \times K$  linear solve.

Section 2 reviews block encoding in QSVT, the polynomial approximation problem, and the three aforementioned base polynomials. Section 3 introduces the pure *spectral polynomial* where we disregard the base polynomials and construct a polynomial that exactly interpolates all the  $N$  eigenvalues as a minimum- $L^2$ -norm solution to an under-determined system. This, however, suf-

fers from several deficiencies. Section 4 presents a more practical *spectrally corrected* method that provides eigenvalue corrections to a base polynomial, leading to spectral-Remez, spectral-Mang, and spectral-Sundërhauf polynomials. Section 5 presents several numerical experiments involving these spectrally corrected polynomials in QSVT. Section 6 discusses the scope, limitations, and future directions of this work. This is followed by conclusions in Section 7.

## 2 Technical Background

### 2.1 Block encoding

A *block encoding* of  $\mathbf{A} \in \mathbb{R}^{N \times N}$  is a unitary  $U_{\mathbf{A}} \in \mathbb{C}^{2^a N \times 2^a N}$  such that [1]

$$\mathbf{A}/\alpha = (\langle 0^a | \otimes I) U_{\mathbf{A}} (|0^a\rangle \otimes I),$$

where  $a$  is an ancilla qubit count and  $\alpha \geq \|\mathbf{A}\|$  is a sub-normalization factor, and  $\mathbf{A}/\alpha$  appears in the top-left block of  $U_{\mathbf{A}}$ :

$$U_{\mathbf{A}} = \begin{bmatrix} \mathbf{A}/\alpha & \cdot \\ \cdot & \cdot \end{bmatrix}$$

For sparse matrices with at most  $s$  non-zeros per row, a block encoding can be constructed using  $O(s \text{ polylog}(N))$  elementary gates [3].

### 2.2 Polynomial approximation

Besides block encoding, the second critical ingredient in QSVT is a polynomial approximation  $p(x)$  to  $1/x$  over the interval  $[a, 1]$ , where  $a = \lambda_{\min}$ , and  $\lambda_{\min}$  is lowest singular value of  $\mathbf{A}/\alpha$ . Three requirements are imposed on polynomial approximations:

1. **Parity:**  $p(x)$  must be an odd polynomial, i.e.  $p(-x) = -p(x)$ .
2. **Boundedness:**  $|p(x)| \leq 1$  for all  $x \in [-1, 1]$ . In practice, a polynomial  $\hat{p}(x)$  is first constructed to approximate  $1/x$  and then normalized:  $p(x) = \hat{p}(x)/\tau$ , where

$$\tau = \max_{x \in [-1, -a] \cup [a, 1]} |\hat{p}(x)| \quad (1)$$

is the *polynomial subnormalization factor*. The post-selection success probability of QSVT scales as

$$P_{\text{succ}} = \frac{\|p(\mathbf{A})\mathbf{b}\|^2}{\tau^2}, \quad (2)$$

so a large  $\tau$  reduces the probability of obtaining the desired output state upon measurement.

3. **Accuracy:**  $p(x)$  should approximate  $1/x$  to a desired tolerance  $\varepsilon$ :

$$|xp(x) - 1| \leq \varepsilon \quad \forall x \in [a, 1]. \quad (3)$$

Here, we consider three methods for constructing such polynomials: Remez [4], Mang [5], and Sundërhauf [6]. All three methods represent  $p(x)$  in the odd Chebyshev basis:

$$p(x) = \sum_{j=0}^{\lfloor d/2 \rfloor} c_j T_{2j+1}(x), \quad (4)$$

where  $T_k(x) = \cos(k \arccos x)$  are Chebyshev polynomials of the first kind [4]. All three methods satisfy the parity requirement by construction. However, they differ in the minimum degree  $d$  needed to achieve the desired  $\varepsilon$  accuracy, and how the coefficients  $\{c_j\}$  are computed. Remez enforces accuracy in the  $L^\infty$  sense over  $[a, 1]$ ; Mang minimizes an  $L^2$  residual in the  $\theta$ -parametrization, which satisfies (3) in practice, but without a uniform guarantee; and Sundërhauf provides a closed-form analytical certificate for both boundedness and accuracy simultaneously.

#### 2.2.1 Remez polynomial

The Remez algorithm [4], proposed by Remez (1934), finds the polynomial minimizing the maximum error over the continuous interval:

$$p^* = \arg \min_{p \in \mathcal{P}_d^{\text{odd}}} \max_{x \in [a, 1]} |xp(x) - 1|. \quad (5)$$

By the Chebyshev equioscillation theorem [4], the solution achieves the same maximum error at  $d+2$  points in  $[a, 1]$  with alternating signs. The algorithm requires solving increasingly ill-conditioned Vandermonde systems as  $d$  grows. Since  $d$  scales as  $O(\sqrt{\kappa} \log(1/\varepsilon))$ , high- $\kappa$  problems may require extended-precision arithmetic. The equioscillatory property, while optimal for continuous approximation, leaves *no slack*: the error touches  $\varepsilon$  at  $d+2$  points with alternating signs, so any perturbation to the coefficients immediately violates the uniform bound at those points. This will be of relevance in Section 4.

### 2.2.2 Mang polynomial

Mang et al. [5] re-parametrize the problem via  $x = \cos \theta$  and minimize the  $L^2$  residual over  $\theta \in [0, \arccos a]$ :

$$\min_{\mathbf{c}} \int_0^{\arccos a} \left| \cos \theta \sum_{j=0}^{n-1} c_j T_{2j+1}(\cos \theta) - 1 \right|^2 d\theta, \quad (6)$$

which reduces to a linear least-squares problem for the Chebyshev coefficients  $\mathbf{c} \in \mathbb{R}^n$ , discretized on a uniform  $\theta$ -grid. The degree  $d = 2n - 1$  is chosen so that the resulting polynomial satisfies (3). The  $L^2$  objective does not guarantee uniform accuracy: the error  $|xp(x) - 1|$  is not equioscillatory and can peak near  $x = a$ . The degree scales as  $O(\sqrt{\kappa} \log(1/\varepsilon))$  and is not guaranteed to be lower than Remez; the relative degree depends on the specific values of  $\kappa$  and  $\varepsilon$ .

### 2.2.3 Sundërhauf polynomial

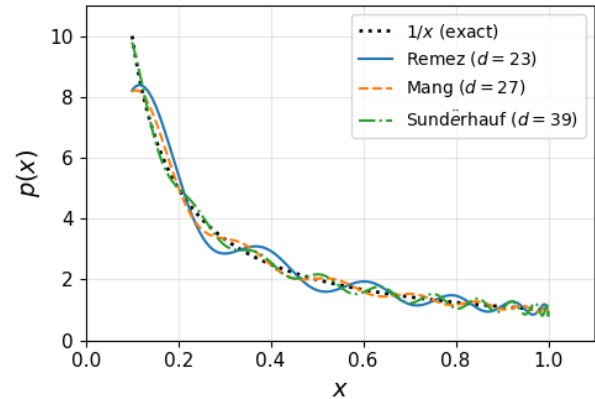
Sundërhauf et al. [6] derive a *closed-form* odd polynomial that natively satisfies the boundedness requirement  $|p(x)| \leq 1$  on  $[-1, 1]$ , without any iterative optimization or linear solve. The polynomial is expressed directly in terms of the problem parameters  $a$  and  $\varepsilon$ , making it the only method among the three that analytically satisfies all three requirements. Furthermore, the method is numerically stable at a high degree, but the degree is often higher than Remez.

### 2.2.4 Comparison

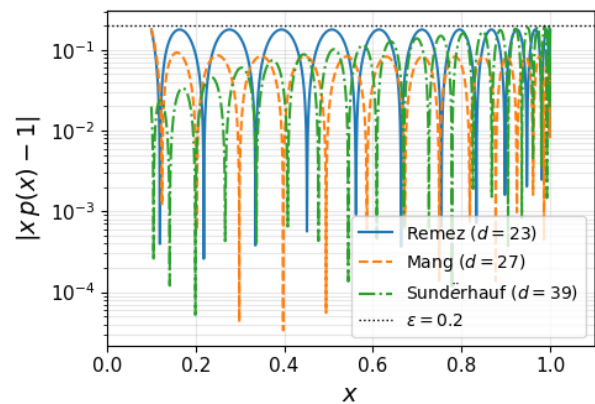
Figure 1a provides a visual comparison of the three approximations for  $\kappa = 10$  and  $\varepsilon = 0.2$ . A large  $\varepsilon$  is used for visual clarity; in practice  $\varepsilon \sim 0.01$ . Remez requires the lowest degree ( $d = 23$ ), followed by Mang ( $d = 27$ ) and then Sundërhauf ( $d = 39$ ). In practice, for typical values of  $\kappa = 100$  and  $\varepsilon = 0.01$ ,  $d$  can exceed 1000.

Figure 1b confirms the theoretical properties of each method. Remez exhibits the classical equioscillation predicted by Chebyshev’s theorem [4]: the error touches  $\varepsilon$  at equal height across  $[a, 1]$ , achieving the minimum possible degree for a given  $\varepsilon$ . Mang shows a similar oscillatory pattern but with peaks slightly higher near  $x = a$ , consistent with the  $L^2$  objective under-weighting the left endpoint. Sundërhauf stays strictly below  $\varepsilon$  everywhere, confirming it is a conservative

analytical bound, with a higher degree ( $d = 39$  vs  $d = 23$  for Remez).



(a) Approximating functions.



(b) Pointwise error.

Figure 1: Polynomial approximation to  $1/x$  for  $\kappa = 10$ ,  $\varepsilon = 0.2$ . (a) Approximation  $p(x)$  vs  $1/x$ . (b) Point-wise error  $|xp(x) - 1|$ : Remez ( $d = 23$ ) achieves a uniform equioscillatory error; Mang ( $d = 27$ ) peaks near  $x = a$ ; Sundërhauf ( $d = 39$ ) satisfies the bound analytically. A large  $\varepsilon$  is used for visual clarity; in practice  $\varepsilon \sim 0.01$ .

## 3 Pure Spectral Polynomial

The three methods reviewed in Section 2.2 share a common philosophy: construct a polynomial that approximates  $1/x$  over the entire continuous interval  $[a, 1]$ . From a QSVT perspective, however, this is stronger than necessary. The QSVT output state is proportional to  $p(\mathbf{A})\mathbf{b} = \sum_k p(\lambda_k)(\mathbf{v}_k^T \mathbf{b})\mathbf{v}_k$ , and the error relative to  $\mathbf{A}^{-1}\mathbf{b} = \sum_k \lambda_k^{-1}(\mathbf{v}_k^T \mathbf{b})\mathbf{v}_k$  depends only on the values  $\{p(\lambda_k)\}$ , not on  $p(x)$  between eigenvalues. The necessary and sufficient accuracy condition is discrete:

$$\max_{k=1, \dots, N} |\lambda_k p(\lambda_k) - 1| \leq \varepsilon. \quad (7)$$

If all  $N$  eigenvalues of  $\mathbf{A}$  are known, the continuous approximation problem reduces to a finite interpolation problem. Let  $p$  be represented in the odd Chebyshev basis with  $n$  terms:

$$p(x) = \sum_{j=0}^{n-1} c_j T_{2j+1}(x).$$

The  $N$  interpolation constraints  $\lambda_k p(\lambda_k) = 1$  form the linear system

$$\underbrace{(\Lambda \mathbf{B})}_{N \times n} \mathbf{c} = \mathbf{1}, \quad (8)$$

where  $B_{kj} = T_{2j+1}(\lambda_k)$  and  $\Lambda = \text{diag}(\lambda_1, \dots, \lambda_N)$ . When  $n > N$  the system is underdetermined; we select the minimum- $\ell^2$ -norm solution via the Moore–Penrose pseudoinverse [7]:

$$\mathbf{c}^* = (\Lambda \mathbf{B})^+ \mathbf{1}. \quad (9)$$

The resulting *spectral polynomial* has degree  $d = 2n - 1$  with  $n = \lceil n_{\text{factor}} \cdot N \rceil$  for a user-chosen ratio  $n_{\text{factor}} \geq 1$ . The minimum-norm solution selects the smoothest polynomial that exactly interpolates  $1/\lambda_k$  at all  $N$  eigenvalues.

Figure 2 illustrates the spectral polynomial for  $\kappa = 10$  with three eigenvalues at  $\lambda = 0.1, 0.5, 1.0$ . At the minimum degree ( $d = 5$ ,  $n_{\text{factor}} = 1$ ), the polynomial interpolates  $1/\lambda_k$  exactly but oscillates between eigenvalues, producing a large  $\tau$  (see 1). As the degree increases, the additional degrees of freedom allow the minimum-norm solution to suppress these oscillations. More importantly, since only the values at the eigenvalues affect the QSVT output, the oscillations do not degrade fidelity — but they inflate  $\tau$  and reduce the success probability  $P_{\text{succ}} \propto 1/\tau^2$ .

While the spectral polynomials exactly interpolate the eigenvalues (and therefore result in zero QSVT error), they suffer from three practical limitations:

- All eigenvalues required.** The polynomial provides no guarantee at uncorrected eigenvalues. If only  $K < N$  eigenvalues are known, the uncontrolled oscillations at uncorrected eigenvalues can destroy solution accuracy.
- Degree grows with  $N$ .** The degree  $d = 2\lceil n_{\text{factor}} \cdot N \rceil - 1$  grows linearly in  $N$ , and the ratio  $n_{\text{factor}}$  required for  $\tau \approx \kappa$  increases with  $\kappa$ , eventually making the degree comparable to the base polynomial degree  $d = O(\sqrt{\kappa} \log(1/\varepsilon))$ .

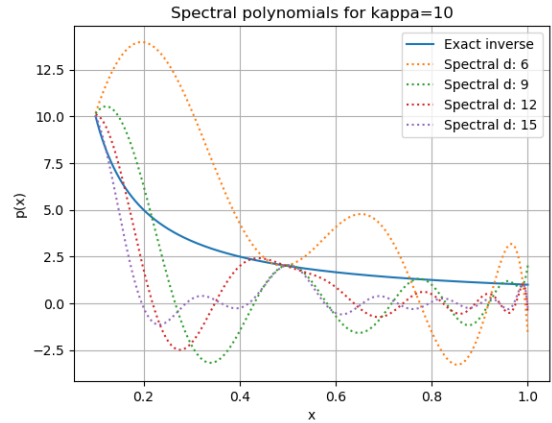


Figure 2: Pure spectral polynomial  $p_S(x)$  for  $\kappa = 10$  with  $N = 3$  eigenvalues at  $\lambda = 0.1, 0.5, 1.0$ , at increasing degree. All polynomials interpolate  $1/\lambda_k$  exactly at the three eigenvalues. As the degree increases, the inter-eigenvalue oscillations diminish and  $\tau$  approaches  $\kappa$ .

- Sensitivity to eigenvalue errors.** Without a continuous approximation guarantee, any discrepancy between the assumed and true eigenvalues produces errors that are unbounded by  $\varepsilon$ . In contrast, a base polynomial ensures  $|\lambda p(\lambda) - 1| \leq \varepsilon$  for all  $\lambda \in [a, 1]$ , regardless of eigenvalue accuracy.

These limitations motivate a correction strategy discussed next: use a base polynomial to provide a continuous safety net, and correct it at the  $K$  eigenvalues that matter most.

## 4 Spectrally Corrected Polynomial

### 4.1 The min-norm correction

A more practical strategy starts from any base polynomial  $p_0$  (Remez, Mang or Sundërhauf) and creates a spectrally corrected polynomial  $p_{SC} = p_0 + p_{\text{corr}}$  that satisfies  $\lambda_k p_{SC}(\lambda_k) = 1$  at the  $K$  smallest eigenvalues  $\lambda_1 \leq \dots \leq \lambda_K$ .

**Remark 4.1.** *Although the proposed correction applies to any subset of eigenvalues, the contiguous  $K$  smallest are preferred for two reasons: (1) if an uncorrected eigenvalue lies between a pair of targeted eigenvalues, the corrected polynomial could exhibit a large error at the uncorrected eigenvalue, and (2) the lowest eigenvalues are often the most critical in many engineering settings.*

The correction polynomial  $p_{\text{corr}}$  is represented

in the same odd Chebyshev basis as  $p_0$ :

$$p_{\text{corr}}(x) = \sum_{j=0}^{n_0-1} \Delta c_j T_{2j+1}(x),$$

where  $\Delta \mathbf{c} \in \mathbb{R}^{n_0}$  is the perturbation to the Chebyshev coefficients. By enforcing the  $K$  constraints, the coefficients are determined as a min-norm correction.

### Spectral correction

**Step 1.** Compute the residuals at the  $K$  smallest eigenvalues:

$$r_k = 1 - \lambda_k p_0(\lambda_k), \quad k = 1, \dots, K.$$

**Step 2.** Solve the  $K \times K$  Gram system for multipliers  $\boldsymbol{\alpha} \in \mathbb{R}^K$ :

$$\begin{aligned} \mathbf{G} \boldsymbol{\alpha} &= \mathbf{r}, \\ G_{ij} &= \lambda_i \lambda_j \sum_{\ell=0}^{n_0-1} T_{2\ell+1}(\lambda_i) T_{2\ell+1}(\lambda_j), \end{aligned} \quad (10)$$

where  $n_0 = (d_0 + 1)/2$  is the number of odd Chebyshev terms in the base polynomial  $p_0$  of degree  $d_0$ .

**Step 3.** Set the correction coefficients and form  $p_{\text{corr}}$ :

$$\begin{aligned} c_j^{\text{corr}} &= \sum_{k=1}^K \alpha_k \lambda_k T_{2j+1}(\lambda_k), \\ j &= 0, \dots, n_0 - 1, \\ p_{\text{corr}}(x) &= \sum_{j=0}^{n_0-1} c_j^{\text{corr}} T_{2j+1}(x). \end{aligned}$$

**Step 4.** Form the corrected polynomial:

$$p_{SC}(x) = p_0(x) + p_{\text{corr}}(x),$$

where  $p_{SC}$  has the **same degree** as  $p_0$  and satisfies  $\lambda_k p_{SC}(\lambda_k) = 1$  exactly for  $k = 1, \dots, K$ .

**Proposition 4.2.** *Let  $p_0$  satisfy  $|x p_0(x) - 1| \leq \varepsilon$  on  $[a, 1]$ , and let  $p_{SC} = p_0 + p_{\text{corr}}$  be the corrected polynomial. Let  $\Lambda_K = \text{diag}(\lambda_1, \dots, \lambda_K)$  and  $\mathbf{B}_K \in \mathbb{R}^{K \times n_0}$  with  $(B_K)_{kj} = T_{2j+1}(\lambda_k)$ . If  $\lambda_k \in [a, 1]$  for all  $k$ , then*

$$|x p_{SC}(x) - 1| \leq \varepsilon + \|\Lambda_K \mathbf{B}_K\| \cdot \|\boldsymbol{\alpha}\|_2 \cdot \|\mathbf{T}(x)\|_2 \quad (11)$$

where  $\mathbf{T}(x) = (T_1(x), T_3(x), \dots, T_{2n_0-1}(x))^T$ .

## 4.2 Degenerate eigenvalues

When the target set contains repeated or nearly repeated eigenvalues — as occurs naturally in problems with spatial symmetry, such as the 2D Poisson equation on a square domain where  $\lambda_{j,k} = \lambda_{k,j}$  — the corresponding rows of  $\Lambda_K \mathbf{B}_K$  are identical, rendering the Gram matrix  $\mathbf{G}$  rank-deficient. The truncated SVD solve handles this algebraically, but the redundant constraints waste degrees of freedom in the correction, producing a larger  $p_{\text{corr}}$  than necessary and potentially degrading uncorrected eigenvalues.

The remedy is straightforward: before applying the correction, merge eigenvalues that are closer than a tolerance  $\delta_{\text{merge}}$ :

$$|\lambda_i - \lambda_j| < \delta_{\text{merge}} \implies \text{retain one representative.} \quad (12)$$

Since a single interpolation constraint  $\lambda_k p_{SC}(\lambda_k) = 1$  applies equally to all eigenmodes sharing the same eigenvalue, duplication removal loses no information. The effective number of constraints  $K_{\text{eff}} \leq K$  equals the number of distinct eigenvalues in the target set.

## 4.3 Illustrative examples

We consider three examples to illustrate the spectrally spectral correction.

**Example 1:** For  $\kappa = 10$ ,  $\varepsilon = 0.2$ , we first construct the three base polynomials: Mang, Remez, and Sundërhauf. We then let  $\lambda_1 = 0.1$ ,  $\lambda_2 = 0.5$ ,  $\lambda_3 = 1.0$ , i.e.,  $K = 3$ , and construct the three corresponding corrected polynomials. In each case,  $p_{SC}$  has the *same degree* as the base polynomial  $p_0$ , and the correction requires solving only a  $3 \times 3$  linear system (10).

Figure 3 shows the point-wise error  $|x p(x) - 1|$  before and after correction for all three base polynomials. In every case the spectral correction reduces the error at the three eigenvalues to machine precision. Between eigenvalues, the spectral error closely tracks the base but increases slightly as expected (consistent with Proposition 4.2). Notably, the spectral-Remez continuous error ( $\varepsilon = 0.36$ ) exceeds that of the base Remez ( $\varepsilon = 0.18$ ), confirming that the equioscillatory profile is most sensitive to perturbation. The spectral-Sundërhauf continuous error ( $\varepsilon = 0.19$ ) remains essentially unchanged, reflecting the margin available in the higher-degree base. However,

recall that errors between eigenvalues do not affect the QSVT output, since the output state  $p(\mathbf{A})\mathbf{b} = \sum_k p(\lambda_k)(\mathbf{v}_k^T \mathbf{b})\mathbf{v}_k$  depends only on the error of  $p$  at the eigenvalues of  $\mathbf{A}$ .

**Example 2:** With the same base polynomials as the previous example, we set the second eigenvalue closer to the lowest:  $\lambda_1 = 0.1$ ,  $\lambda_2 = 0.15$ ,  $\lambda_3 = 1.0$ . Figure 4 shows the point-wise error  $|xp(x) - 1|$  before and after correction for all three base polynomials. While the closely spaced pair  $\lambda_1 = 0.1$ ,  $\lambda_2 = 0.15$  causes a significant increase in the inter-eigenvalue error, this will not affect the QSVT output, which depends on  $p$  only at the eigenvalues. Furthermore, the subnormalization factor increases only modestly from  $\tau_0 \in [8.2, 9.8]$  to  $\tau_{SC} = \kappa = 10.0$  for all three bases, since the correction enforces  $p_{SC}(\lambda_1) = 1/\lambda_1$  exactly. The success probability  $1/\tau^2$  is therefore governed by  $\kappa$  alone, independent of the base polynomial.

**Example 3:** Next, we set the second eigenvalue identical to the first:  $\lambda_1 = 0.1$ ,  $\lambda_2 = 0.1$ ,  $\lambda_3 = 1.0$ , to illustrate the effect of degenerate eigenvalues. The duplication removal procedure of Section 4.2 merges the repeated pair, reducing the effective correction to  $K_{\text{eff}} = 2$  distinct eigenvalues. Figure 5 shows the point-wise error  $|xp(x) - 1|$ . The results are visually identical to Example 1 ( $\lambda = 0.1, 0.5, 1.0$  with  $K = 3$ ), confirming that duplication removal correctly handles repeated eigenvalues without degradation.

## 5 Numerical Experiments

Having established the polynomial-level behavior of the spectral correction, we now validate the proposed formulations on 1D and 2D Poisson problems.

### 5.1 1D and 2D Poisson Finite Difference

For convenience, we provide here the well-known analytical expressions for the eigenvalues of finite difference formulations of 1D and 2D Poisson problems.

For the 1D Poisson equation  $-u'' = f$  on  $(0, 1)$  with Dirichlet boundary conditions, discretized on  $N$  interior nodes with  $h = 1/(N + 1)$ , the

eigenvalues are [7]

$$\lambda_k = \frac{4}{h^2} \sin^2\left(\frac{k\pi}{2(N+1)}\right), \quad k = 1, \dots, N, \quad (13)$$

with condition number  $\kappa \approx \frac{4}{\pi^2}(N+1)^2$ .

For the 2D Poisson equation  $-\nabla^2 u = f$  on  $(0, 1)^2$  with Dirichlet boundary conditions, discretized with  $N_1$  interior nodes per direction ( $N = N_1^2$ ), the eigenvalues are pairwise sums of the 1D eigenvalues [7]:

$$\lambda_{j,k} = \frac{4}{h^2} \left[ \sin^2\left(\frac{j\pi}{2(N_1+1)}\right) + \sin^2\left(\frac{k\pi}{2(N_1+1)}\right) \right], \quad j, k = 1, \dots, N_1, \quad (14)$$

with the same condition number  $\kappa \approx \frac{4}{\pi^2}(N_1+1)^2$  as the 1D case.

In both cases, the normalized eigenvalues  $\tilde{\lambda} = \lambda/\lambda_{\max}$  satisfy  $\tilde{\lambda} \in (0, 1]$  with  $\tilde{\lambda}_{\min} = 1/\kappa$ .

### 5.2 QSVT Metrics

Given the block-encoded matrix  $\mathbf{A}$  and a polynomial approximation to  $1/x$ , the QSP phase angles  $\{\phi_j\}_{j=0}^d$  are computed via the `pyqsp` package [1, 8], and the resulting quantum circuit is simulated via *noiseless statevector* simulation in Qiskit [9].

If  $\mathbf{u} = \mathbf{A}^{-1}\mathbf{b}/\|\mathbf{A}^{-1}\mathbf{b}\|$  denotes the normalized classical solution and  $\mathbf{u}_{\text{QSVT}}$  the normalized QSVT output, the output state fidelity is

$$F = \left| \mathbf{u}^\top \mathbf{u}_{\text{QSVT}} \right|^2, \quad (15)$$

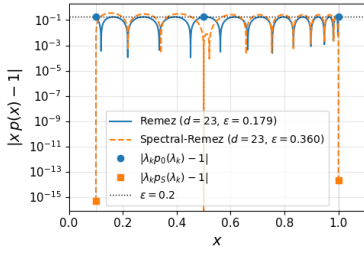
The classical compliance  $C = \mathbf{b}^\top \mathbf{A}^{-1}\mathbf{b}$  and the QSVT compliance is recovered as

$$C_{\text{QSVT}} = (\mathbf{b}^\top \mathbf{u}_{\text{QSVT}}) \tau \sqrt{P_{\text{succ}}}, \quad (16)$$

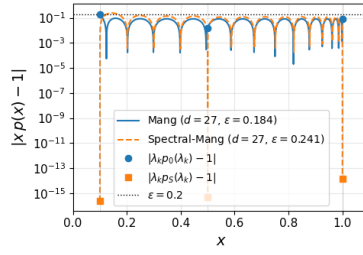
where  $\tau$  is the polynomial subnormalization factor (1), and  $P_{\text{succ}}$  is the post-selection success probability (2). The relative compliance error  $|C_{\text{QSVT}} - C|/|C|$  provides a physically meaningful scalar measure of solution accuracy, in addition to the state fidelity  $F$ .

### 5.3 Pure Spectral Polynomial

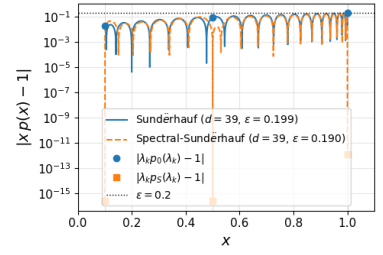
We first assess the pure spectral polynomial  $p_S$  of Section 3, which requires all  $N$  eigenvalues and is applicable when  $N$  is small. Table 1 reports



(a) Remez and Spectral-Remez.

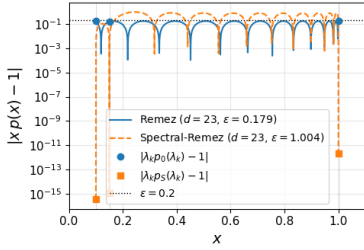


(b) Mang and Spectral-Mang.

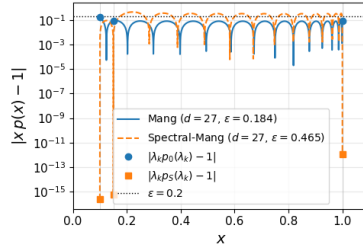


(c) Sundérhauf and Spectral-Sundérhauf.

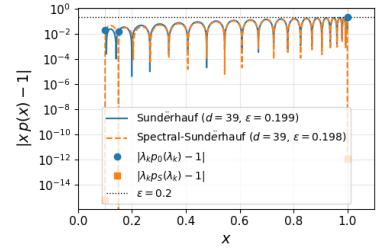
Figure 3: Spectral correction applied to three base polynomials ( $\kappa = 10$ ,  $\varepsilon = 0.2$ ,  $K = 3$  eigenvalues at  $\lambda = 0.1, 0.5, 1.0$ ). In all cases the spectrally corrected polynomial  $p_{SC}$  achieves machine-precision errors at the eigenvalues, while preserving the continuous error profile of the base polynomial, at no increase in degree.



(a) Remez and Spectral-Remez.

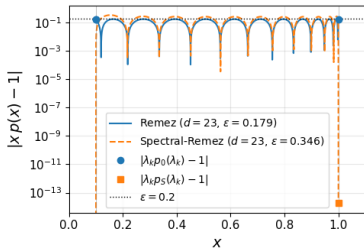


(b) Mang and Spectral-Mang.

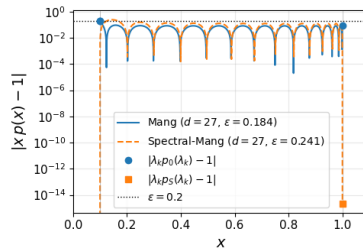


(c) Sundérhauf and Spectral-Sundérhauf.

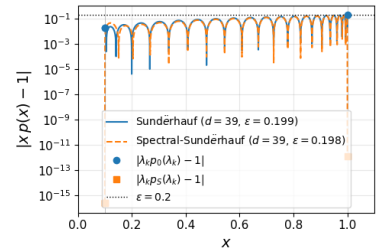
Figure 4: Spectral correction applied to three base polynomials ( $\kappa = 10$ ,  $\varepsilon = 0.2$ ,  $K = 3$  eigenvalues at  $\lambda = 0.1, 0.15, 1.0$ ). The spectrally corrected polynomial achieves machine-precision errors at the eigenvalues, but the closely spaced eigenvalues cause a perceptible increase in the inter-eigenvalue error.



(a) Remez and spectral-Remez.



(b) Mang and spectral-Mang.



(c) Sundérhauf and spectral-Sundérhauf.

Figure 5: Spectral correction with a degenerate eigenvalue pair ( $\kappa = 10$ ,  $\varepsilon = 0.2$ ,  $\lambda = 0.1, 0.1, 1.0$ ,  $K_{\text{eff}} = 2$  after duplication removal). The correction achieves machine-precision errors at both distinct eigenvalues, with the continuous error profile matching Example 1.

Table 1: Pure spectral polynomial for the 1D Poisson equation. All cases achieve unit fidelity ( $F = 1.000000$ ) with uniform load; only  $\tau/\kappa$  and the success probability vary.

$n_{\text{factor}}$	$m = 3$ ( $N = 8, \kappa = 32.5$ )			$m = 4$ ( $N = 16, \kappa = 117.6$ )		
	$d$	$\tau/\kappa$	$P_{\text{succ}}$	$d$	$\tau/\kappa$	$P_{\text{succ}}$
2	31	1.41	0.577	63	28.5	0.324
3	47	1.25	0.728	95	1.63	0.500
4	63	1.01	0.929	127	1.39	0.533
5	79	1.01	0.967	159	1.30	0.663
8	127	1.00	0.979	255	1.00	0.887

the degree– $\tau$  trade-off for the 1D Poisson problem with  $m = 3$  ( $N = 8, \kappa = 32.5$ ) and  $m = 4$  ( $N = 16, \kappa = 117.6$ ).

For  $m = 3$ ,  $n_{\text{factor}} = 4$  ( $d = 63$ ) suffices to reach  $\tau \approx \kappa$ . For  $m = 4$ ,  $n_{\text{factor}} = 8$  ( $d = 255$ ) is required — comparable to the base Mang degree at  $\varepsilon = 0.2$  ( $d = 305$ ). This confirms the second limitation of Section 3: the  $n_{\text{factor}}$  needed for  $\tau \approx \kappa$  grows with  $\kappa$ , eventually eroding the degree advantage over base polynomials.

The pure spectral polynomial is therefore most effective for small problems where all eigenvalues are known and  $\kappa$  is moderate. For larger or higher- $\kappa$  problems, the spectrally corrected approach of the following subsections is preferred.

## 5.4 Spectrally Corrected Polynomials

### 5.4.1 1D Poisson Polynomial Error

We set  $K = N = 4$ , using all eigenvalues of the 1D Poisson FD matrix with  $N = 4$  interior nodes ( $\kappa = 9.47, \varepsilon = 0.1$ ):  $\lambda_1 = 0.1056, \lambda_2 = 0.3820, \lambda_3 = 0.7236, \lambda_4 = 1.0$ . Figure 6 shows that spectral correction for all three base polynomials achieve machine-precision errors at all four eigenvalues, with the spectral error closely tracking the base between eigenvalues. This confirms that when the full eigenvalue spectrum is available and well-separated, the spectral correction is effective regardless of the choice of base polynomial.

### 5.4.2 Degree–accuracy trade-off

A central benefit of the spectral correction is that it achieves machine-precision eigenvalue accuracy at a much lower degree than a base polynomial. Eigenvalue accuracy is measured via the maxi-

mum eigenvalue residual:

$$\mathcal{E}_{\text{eig}} = \max_k |\lambda_k p(\lambda_k) - 1|. \quad (17)$$

For brevity, we use Mang as a base polynomial in this experiment; results for Remez and Sunderhauf are qualitatively similar. Table 2 makes the central claim explicit for  $N = 4$  ( $\kappa \approx 9.47$ ) with  $K = 2 = N/2$  corrected eigenvalues.

Table 2: Degree  $d$  and maximum eigenvalue residual  $\mathcal{E}_{\text{eig}} = \max_k |\lambda_k p(\lambda_k) - 1|$  for Mang and spectral-Mang at increasing accuracy targets.  $N = 4, \kappa \approx 9.47, K = 2$ . Two columns report  $\mathcal{E}_{\text{eig}}$  at the  $K$  corrected eigenvalues and over the full spectrum respectively.

Method	$\varepsilon$	$d$	$\mathcal{E}_{\text{eig}} (K \text{ corr.})$	$\mathcal{E}_{\text{eig}} (\text{all } N)$
Mang	0.2	25	$1.92 \times 10^{-1}$	$1.92 \times 10^{-1}$
Mang	0.1	33	$9.27 \times 10^{-2}$	$9.27 \times 10^{-2}$
Mang	0.01	57	$9.05 \times 10^{-3}$	$9.05 \times 10^{-3}$
Spectral-Mang ( $K = 2$ )	0.2	25	$2.22 \times 10^{-16}$	$1.58 \times 10^{-1}$
Spectral-Mang ( $K = 2$ )	0.1	33	$1.11 \times 10^{-16}$	$1.51 \times 10^{-2}$
Spectral-Mang ( $K = 2$ )	0.01	57	$1.00 \times 10^{-16}$	$2.71 \times 10^{-3}$

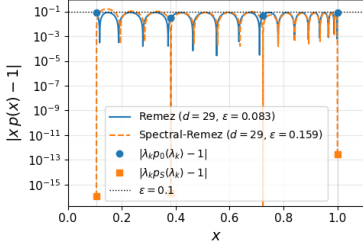
Two observations follow from Table 2. First, spectral-Mang with  $K = 2$  achieves machine-precision residuals at the corrected eigenvalues, regardless of  $\varepsilon$ , while the base polynomial requires  $\varepsilon \rightarrow 0$  (and correspondingly higher degree) to approach the same accuracy. Second, the uncorrected eigenvalues retain the accuracy of the base polynomial, consistent with Proposition 4.2.

### 5.4.3 QSVT validation for 1D Poisson

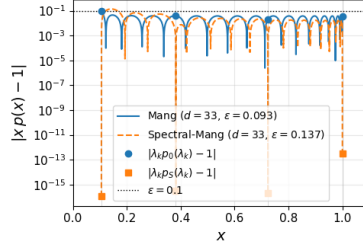
We now validate the full QSVT pipeline using the spectrally corrected polynomial.

Table 3 reports results for  $m = 4$  ( $N = 16, \kappa = 117.6$ ) with  $K = N = 16$  corrected eigenvalues, using the Mang base polynomial. Two load cases are shown: a uniform load (smooth, low-frequency dominated) and a point load at the midpoint (broadband, all modes excited).

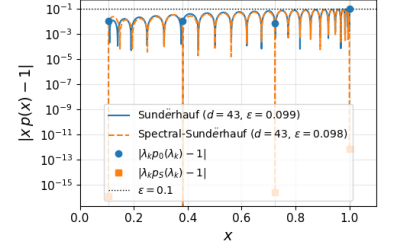
The spectral correction achieves unit fidelity for both load cases at  $\varepsilon = 0.5$ , matching the tight reference ( $\varepsilon = 10^{-3}$ ) at  $5.28 \times$  lower circuit depth ( $d = 177$  vs  $d = 935$ ). The compliance error is an order of magnitude better than the tight reference for the uniform load ( $3.73 \times 10^{-5}$  vs  $5.78 \times 10^{-4}$ ) and comparable for the point load ( $1.04 \times 10^{-4}$  vs  $5.25 \times 10^{-4}$ ). The success probability of the spectrally corrected methods is comparable to the loose base despite a larger polynomial subnormalization factor  $\tau$ , because the im-



(a) Remez and Spectral-Remez.



(b) Mang and Spectral-Mang.



(c) Sundërhauf and Spectral-Sundërhauf.

Figure 6: Spectral correction using all  $K = 4$  eigenvalues of the 1D Poisson FD matrix with  $N = 4$  interior nodes ( $\kappa = 9.47$ ,  $\varepsilon = 0.1$ ,  $\lambda_1 = 0.106$ ,  $\lambda_2 = 0.382$ ,  $\lambda_3 = 0.724$ ,  $\lambda_4 = 1.0$ ).

Table 3: QSVT results for the 1D Poisson equation,  $m = 4$  ( $N = 16$ ,  $\kappa = 117.6$ ),  $K = N = 16$ , Mang base. The spectrally corrected method at  $\varepsilon = 0.5$  achieves unit fidelity and lower compliance error than the tight reference at  $5.28 \times$  lower circuit depth.

Method	$d$	Fidelity	Rel. compl. err	$P_{\text{succ}}$	$\tau$
<i>Uniform load</i>					
Mang ( $\varepsilon = 0.5$ )	177	0.999536	$4.91 \times 10^{-1}$	0.772	74.4
Mang ( $\varepsilon = 10^{-3}$ )	935	1.000000	$5.78 \times 10^{-4}$	0.717	156.2
Spectral-Mang ( $\varepsilon = 0.5$ )	177	1.000000	$3.73 \times 10^{-5}$	0.781	142.8
<i>Point load at midpoint</i>					
Mang ( $\varepsilon = 0.5$ )	177	0.991581	$4.09 \times 10^{-1}$	0.667	74.4
Mang ( $\varepsilon = 10^{-3}$ )	935	1.000000	$5.25 \times 10^{-4}$	0.627	156.2
Spectral-Mang ( $\varepsilon = 0.5$ )	177	1.000000	$1.04 \times 10^{-4}$	0.664	142.8

proved polynomial accuracy increases the numerator  $\|p_{SC}(\mathbf{A})\mathbf{b}\|^2$  proportionally. Spectral-Remez and spectral-Sundërhauf yield qualitatively identical results and are not included here for brevity.

#### 5.4.4 Robustness to eigenvalue perturbations

In practice, eigenvalues may be known only approximately, for example via a Lanczos iteration rather than the closed-form expression (13). We assess robustness by replacing the exact eigenvalues  $\lambda_k$  with perturbed values  $\hat{\lambda}_k = \lambda_k(1 + \delta_k)$ ,  $\delta_k \sim \mathcal{U}(-\eta, \eta)$ , and repeating the QSVT experiment of Section 5.4.3, for the uniform load case, with  $n = 10$  independent trials per perturbation level. Table 4 reports the mean and standard deviation of fidelity and relative compliance error.

Table 4: Robustness of spectral-Mang to eigenvalue perturbations.  $m = 4$  ( $N = 16$ ,  $\kappa = 117.6$ ),  $K = N = 16$ ,  $\varepsilon = 0.5$ ,  $n = 10$  trials per perturbation level  $\eta$ .

$\eta$	Fidelity	Rel. compl. err	$P_{\text{succ}}$
0 (exact)	1.000000	$1.56 \times 10^{-4}$	0.821
$10^{-2}$	$1.000000 \pm 3 \times 10^{-7}$	$3.32 \times 10^{-3} \pm 5 \times 10^{-3}$	0.821
$10^{-1}$	$0.999808 \pm 3 \times 10^{-4}$	$1.81 \times 10^{-2} \pm 4 \times 10^{-2}$	0.822

Fidelity remains at unity to five decimal places at  $\eta = 10^{-2}$ , and even at  $\eta = 10^{-1}$ , the fidelity loss is below  $2 \times 10^{-4}$  and the compliance error remains below  $2 \times 10^{-2}$ . The success probability is unaffected by eigenvalue perturbation, confirming that  $\tau$  depends only on the base polynomial.

#### 5.4.5 QSVT validation for 2D Poisson

A uniform load is used as the forcing function for the 2D Poisson problem and a full QSVT pipeline is executed. Table 5 reports fidelity and peak solution value for spectral-Mang at  $\varepsilon = 0.2$  ( $d = 305$ ) with increasing  $K$ . The base Mang polynomial already achieves high fidelity (0.99987) for this smooth load; the spectral correction pushes fidelity to 0.999996 at  $K = 32$  ( $K_{\text{eff}} = 18$  after removing duplicates), recovering the classical peak value to within 0.02%.

Unlike the 1D case where  $K = N$  corrects the full spectrum, the 2D problem has  $N = N_1^2$  eigenvalues but the polynomial has only  $n_0 = (d + 1)/2 = 153$  odd Chebyshev terms, limiting the effective number of corrections to  $K \ll n_0$ . In practice, correcting the  $K \approx 8\text{--}16$  smallest eigenvalues — where the base polynomial error is largest — suffices to achieve fidelity above 0.9999.

Table 5: Spectral-Mang on the 2D Poisson equation ( $N = 256$ ,  $\kappa = 117.6$ ,  $\varepsilon = 0.2$ ,  $d = 305$ , uniform load). Classical peak value: 0.1044.

$K$	$K_{\text{eff}}$	Fidelity	Max value	Peak error
0 (base)	—	0.99987	0.1033	−1.1%
1	1	0.99969	0.1071	+2.5%
4	3	0.99941	0.1081	+3.5%
8	5	0.99997	0.1040	−0.4%
16	10	0.999998	0.1046	+0.2%
32	18	0.9999996	0.1044	+0.0%

Figure 7 shows the solution surfaces for the classical, base Mang, and spectral-Mang ( $K = 32$ ) cases.

## 6 Discussion

### 6.1 Scope and limitations

The approach is most effective for structured discretizations where eigenvalues are available analytically, such as FD and FEM on uniform grids. For unstructured meshes, a preprocessing step (Lanczos or QPE) is required, and its cost must be weighed against the QSVT benefit.

Furthermore, when eigenvalues are obtained approximately, the correction enforces  $\hat{\lambda}_k p_{SC}(\hat{\lambda}_k) = 1$  exactly at the *supplied* values, not at the true eigenvalues of  $\mathbf{A}$ . The accuracy of the QSVT output, therefore, depends on how closely  $\hat{\lambda}_k$  approximates  $\lambda_k$ . The perturbation experiment of Section 5.4.4 quantifies this dependence: errors up to  $\eta = 10\%$  degrade the compliance error proportionally while fidelity loss remains below  $2 \times 10^{-5}$ .

### 6.2 Relation to classical polynomial preconditioning

Exploiting eigenvalue estimates to accelerate linear solvers has a long history in classical polynomial preconditioning [10–14]. The spectral correction presented here is the natural QSVT analogue: eigenvalue knowledge is used to shape the polynomial, thereby improving accuracy at a fixed circuit depth. The main difference is that, in a classical setting, polynomial preconditioning has largely been replaced by more efficient preconditioners such as ILU. On the other hand, in the QSVT setting, polynomial approximation is mandatory, making spectral adaptation both natural and necessary. Furthermore, classical polynomial preconditioning relies on eigenvalue estimates; we have exploited exact, closed-form expressions to establish the method and its limits. When closed-form eigenvalues are unavailable, the perturbation experiment of Section 5.4.4 suggests that approximate eigenvalues may suffice.

### 6.3 Future directions

**Parameter sensitivity:** The interplay between the base tolerance  $\varepsilon$ , the number of corrected eigenvalues  $K$ , the polynomial degree  $d$ , and the eigenvalue density of the operator warrants further investigation. The 2D experiments in Section 5.4.5 suggest that denser spectra require tighter base tolerances to avoid degrading uncorrected eigenvalues, but a systematic characterization of this trade-off remains open.

**Extension to FEM and elasticity operators:** The experiments in this paper use finite difference discretizations of the Poisson equation. Extending the spectral correction to finite element discretizations and to the Lamé equations of linear elasticity is a natural next step. For operators with tensor-product structure, closed-form eigenvalues are available.

**Lanczos and QPE eigenvalue extraction:** For operators without closed-form eigenvalues, a short Lanczos run ( $\sim 20$  steps) provides the  $K$  smallest Ritz values to  $\sim 0.1\%$  accuracy [7], sufficient for the spectral correction given its demonstrated robustness to eigenvalue perturbations. Alternatively, quantum phase estimation can extract eigenvalues from the block encoding directly, amortizing the cost over multiple solves and eliminating the classical preprocessing step entirely.

**Spectral extension:** An alternative to the spectral correction is *spectral extension* where we extend the base polynomial by  $K$  new odd Chebyshev terms of degree  $d_0 + 2, d_0 + 4, \dots, d_0 + 2K$ , using those additional degrees of freedom exclusively to satisfy the  $K$  interpolation constraints. This preserves the continuous error profile of the base polynomial exactly — including the equioscillation of the Remez polynomial — at the cost of increasing the degree by  $2K$ . The square  $K \times K$  system is solved for the new coefficients alone, leaving the existing coefficients untouched. Spectral extension and spectral correction fall under the umbrella of *spectral bootstrapping*: exploiting eigenvalue knowledge to improve QSVT polynomials.

**QSVT on near-term hardware:** The circuit depth reductions demonstrated here (up to  $5.28\times$

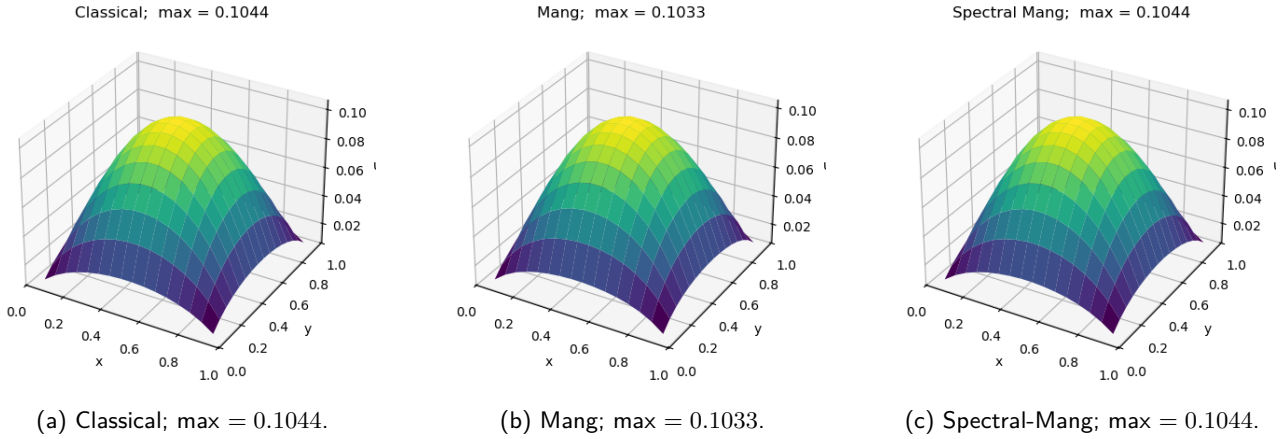


Figure 7: 2D Poisson solution surfaces ( $N = 256$ ,  $\kappa = 117.6$ , uniform load,  $\varepsilon = 0.2$ ,  $d = 305$ ). Spectral-Mang with  $K = 32$  ( $K_{\text{eff}} = 18$ ) recovers the classical solution.

for the 1D Poisson problem) directly reduce error accumulation on near-term hardware. Combining the spectral correction with zero-noise extrapolation [15] could further close the gap between statevector fidelity and hardware fidelity, making QSVT of small Poisson instances ( $N = 4$ ,  $d = 25$ ) tractable on current quantum devices.

## 7 Conclusion

We have presented a framework for reducing polynomial degree — and hence quantum circuit depth — in QSVT-based linear solvers by exploiting prior knowledge of the matrix spectrum.

The key observation is that QSVT solution accuracy depends only on the polynomial values at the eigenvalues of  $\mathbf{A}$ , not between them. When all  $N$  eigenvalues are known, a pure spectral polynomial achieves unit fidelity at reduced degree, but has practical limitations.

To address these limitations, we propose the *spectral correction*: given any base polynomial  $p_0$  of degree  $d_0$  and  $K \leq N$  known eigenvalues, a  $K \times K$  Gram system enforces exact interpolation at those eigenvalues without increasing  $d_0$ . The corrected polynomial  $p_{SC}$  achieves machine-precision residuals at the corrected eigenvalues regardless of the base tolerance  $\varepsilon$ , while the base polynomial provides a continuous safety net at uncorrected eigenvalues.

QSVT experiments on the 1D Poisson equation ( $N = 16$ ,  $\kappa = 117.6$ ) demonstrate up to a  $5.28\times$  reduction in circuit depth relative to a base Mang polynomial, at unit fidelity and improved compliance error. Spectral correction is

agnostic to the choice of base polynomial and robust to eigenvalue perturbations up to 10% relative error. Extension to the 2D Poisson equation ( $N = 256$ ) confirms that correcting a small fraction of the spectrum ( $K_{\text{eff}} = 10$  of 256 eigenvalues) suffices to achieve fidelity above 0.999, with degenerate eigenvalues handled via duplication removal. Future directions include extension to FEM and elasticity operators, systematic characterization of the tolerance–density trade-off, and Lanczos/QPE eigenvalue extraction as outlined in Section 6.3.

## Acknowledgments

The author would like to acknowledge the Vilas Associate Grant from the University of Wisconsin Graduate School.

## Declarations

The author declares no conflict of interest.

## Code reproducibility and availability

The QSP phase computation is sensitive to the numerical linear algebra backend; all experiments use NumPy 2.3.5 and SciPy 1.15.3. The code developed in this work is available at <https://github.com/UW-ERSL/SpectralCorrectionQSVT.git> and will be made public upon publication.

## References

- [1] András Gilyén, Yuan Su, Guang Hao Low, and Nathan Wiebe. Quantum singular value transformation and beyond: exponential improvements for quantum matrix arithmetics. *Proceedings of the 51st Annual ACM STOC*, pages 193–204, 2019. DOI: [10.1145/3313276.3316366](https://doi.org/10.1145/3313276.3316366).
- [2] John M Martyn, Zane M Rossi, Andrew K Tan, and Isaac L Chuang. Grand unification of quantum algorithms. *PRX quantum*, 2(4):040203, 2021.
- [3] Andrew M. Childs, Robin Kothari, and Rolando D. Somma. Quantum algorithm for systems of linear equations with exponentially improved dependence on precision. *SIAM Journal on Computing*, 46(6):1920–1950, 2017. DOI: [10.1137/16M1087072](https://doi.org/10.1137/16M1087072).
- [4] Lloyd N. Trefethen. *Approximation Theory and Approximation Practice, Extended Edition*. Society for Industrial and Applied Mathematics, Philadelphia, 2019. DOI: [10.1137/1.9781611975949](https://doi.org/10.1137/1.9781611975949).
- [5] Chetra Mang, Sunheang Ty, Axel Tahmasebimoradi, Renaud Vilmart, and Rim Kadah. Numerical experiments using block-diagonalization technique for solving Poisson’s equation. In *Quantum Engineering Sciences & Technologies for Industry & Services (QUEST)*, Saclay, France, December 2025. HAL: hal-05269586.
- [6] Christoph Sünderhauf, Earl Campbell, and Daan Camps. Block-encoding structured matrices for data input in quantum computing. In *Quantum*, volume 8, page 1226, 2024. DOI: [10.22331/q-2024-01-11-1226](https://doi.org/10.22331/q-2024-01-11-1226).
- [7] Gene H. Golub and Charles F. Van Loan. *Matrix Computations*. Johns Hopkins University Press, Baltimore, 4th edition, 2013.
- [8] Jeongwan Haah. Product decomposition of periodic functions in quantum signal processing. *Quantum*, 3:190, 2019. DOI: [10.22331/q-2019-10-07-190](https://doi.org/10.22331/q-2019-10-07-190).
- [9] Ali Javadi-Abhari, Matthew Treinish, Kevin Krsulich, Christopher J Wood, Jake Lishman, Julien Gacon, Simon Martiel, Paul D Nation, Lev S Bishop, Andrew W Cross, et al. Quantum computing with qiskit. *arXiv preprint arXiv:2405.08810*, 2024.
- [10] Bernd Fischer and Roland W. Freund. On adaptive weighted polynomial preconditioning for Hermitian positive definite matrices. *SIAM Journal on Scientific Computing*, 15(2):408–426, 1994. DOI: [10.1137/0915028](https://doi.org/10.1137/0915028).
- [11] Steven F. Ashby, Thomas A. Manteuffel, and James S. Otto. A comparison of adaptive Chebyshev and least squares polynomial preconditioning for Hermitian positive definite linear systems. *SIAM Journal on Scientific and Statistical Computing*, 13(1):1–29, 1992.
- [12] Yousef Saad. Practical use of polynomial preconditionings for the conjugate gradient method. *SIAM Journal on Scientific and Statistical Computing*, 6(4):865–881, 1985.
- [13] Jennifer A. Loe and Ronald B. Morgan. Toward efficient polynomial preconditioning for GMRES. *Numerical Linear Algebra with Applications*, 29(4):e2427, 2022.
- [14] Feng Zhang, Xuebin Chi, Jinrong Jiang, Junlin Wei, Lian Zhao, and Yuzhu Wang. An efficient scaling scheme for polynomial acceleration in ilu-preconditioned systems. *Concurrency and Computation: Practice and Experience*, 37(9-11):e70098, 2025.
- [15] Kristan Temme, Sergey Bravyi, and Jay M. Gambetta. Error mitigation for short-depth quantum circuits. *Physical Review Letters*, 119(18):180509, 2017. DOI: [10.1103/PhysRevLett.119.180509](https://doi.org/10.1103/PhysRevLett.119.180509).